Ninth Canadian Conference on
Earthquake Engineering
Ottawa, Ontario, Canada
26-29 June 2007

INFLUENCE OF GROUND MOTION ON EFFECTIVE STIFFNESS OF HIGH-RISE CANTILEVER WALLS

P. Adebar[1], A. Korchinski[2] and T. Haukaas[3]

ABSTRACT

Nonlinear dynamic analysis was used to study the influence of ground motions on the effective stiffness of a high-rise cantilever wall. To simplify the analyses, a simplified force–displacement model for high-rise cantilever walls was first developed from the results of a fibre model, a simplified trilinear bending moment – curvature model, and the results from a large-scale test of a cantilever wall. The model consists of a rational predefined envelope, and empirical hysteretic rules. If the effective stiffness of the particular wall that was studied is determined from the elastic stiffness of an equivalent bi-linear load-displacement relationship with equal area-under-the-curve, the stiffness reduction factor $\alpha = k_e / k_g$ should be taken as 80%. While the influence of the particular ground motion is very significant, the average results from the nonlinear dynamic analysis suggests that the stiffness reduction factor reduces gradually from about 85% or 90% at R = 1.5 to a reduction factor of about 60% at an R = 5.0.

Introduction

According to the National Building Code of Canada, linear dynamic analysis of concrete structures must be done using a structural model that accounts for the effect of cracked sections. Similarly, the seismic design provisions of the Canadian concrete code requires that the design displacement be determined accounting for cracked sections. The design displacement is needed to check if confinement is required in the plastic hinge region of a concrete wall, to determine the shear strength of a ductile concrete wall, to determine the rotational demands on coupling beams, and to determine the punching shear capacity of slab-column connections in gravity load frames attached to the SFRS.

The flexural rigidity of an uncracked concrete wall is usually assumed to be $E_c I_g$, where E_c is the Modulus of Elasticity of concrete and I_g is the second moment of area of the gross concrete section. When a concrete wall is subjected to significant earthquake actions, the wall cracks and the flexural stiffness reduces in the vicinity of the cracks. To account for the reduction in stiffness in linear analysis, an effective flexural rigidity $E_c I_e = \alpha E_c I_g$ is used. A single reduction factor $\alpha = I_e / I_g$ is normally used for an entire concrete wall. This reduction factor is an average value accounting for the variation of cracking as a wall is subjected to increasing force, the variation of cracking over the height of the wall, and the variation of stiffness at cracked and uncracked sections. FEMA 356 recommends a factor of 80% for previously uncracked concrete walls and a factor of 50% for previously cracked walls. The commentary to the 1995

[1] Professor, Dept. of Civil Engineering, University of British Columbia, Vancouver, BC, V6T 1Z4.
[2] Graduate Research Assistant, Dept. of Civil Engineering, University of British Columbia, Vancouver, BC, V6T 1Z4.
[3] Assistant Professor, Dept. of Civil Engineering, University of British Columbia, Vancouver, BC, V6T 1Z4.

New Zealand concrete code, recommends a factor of 25% for a concrete wall with no axial force and a factor of 35% for a concrete wall with an axial compression force equal to 10% $f_c'A_g$.

Upper-bound and Lower-bound Effective Stiffness

The most general model for calculating nonlinear flexural response of any reinforced concrete section is a fibre (layer) model, in which stress-strain relationships for concrete and reinforcement are used to determine the stress in fibres (layers) of the cross-section at a given strain level. The stress-strain response of concrete and post-yielding stress-strain response of reinforcement depend on strain history. Thus the cyclic flexural response of reinforced concrete depends on the maximum strains reached in previous load cycles. Rather than deal with an infinite number of bending moment – curvature relationships depending on previous load history, the concept of an upper-bound and lower-bound bending moment – curvature response can be used. The upper-bound response corresponds to a previously uncracked wall that is loaded monotonically to failure, while the lower-bound response corresponds to a wall that is severely cracked during previous load cycles.

Adebar and Ibrahim (2002) used the results from a fibre model to develop a simple nonlinear flexural model for typical high-rise concrete shear walls where the nonlinear compression strains of concrete are relatively small. They proposed that both the upper-bound and lower-bound bending moment – curvature relationships of a typical concrete shear wall can be reasonably approximated by trilinear curves. The trilinear bending moment – curvature model was used to develop a general method for estimating the upper-bound and lower-bound effective flexural rigidity of concrete walls accounting for the magnitude of axial compression, amount and distribution of vertical reinforcement, concrete geometry, and all parameters that affect the flexural capacity of the wall (Ibrahim and Adebar 2004). The effective flexural stiffness was determined from the slope of the elastic portion of an equivalent elastic-plastic load-displacement curve that has the same area under the curve as the actual nonlinear relationship. A wide range of different walls were examined, and it was observed that the parameter that most influences the effective moment of inertia is the axial compression applied at the base of the wall. Thus simplified expressions were proposed by Ibrahim and Adebar (2002) for the upper-bound and lower-bound effective moment of inertia of concrete shear walls.

In order to validate the models described above, Adebar et al. (n.d) conducted a large-scale test on a slender concrete wall. A 12.5 m (41 ft) "high" concrete wall with a height-to-length ratio of 7.6 was constructed and tested in a horizontal position supported on sliding bearings. The wall had a flanged cross section, low percentage of vertical reinforcement (0.65% in the flanges and 0.25% in the web), and was subjected to a uniform axial compression equal to 0.10 $f_c'A_g$ in addition to a reverse cyclic lateral point load applied at 11.33 m (37 ft) from the critical flexural section. The envelopes of the measured load-displacement relationships were converted to an equivalent bi-linear load-displacement relationship with equal area-under-the-curve up to the point that the non-linear curves cross the nominal capacity. This procedure suggests an effective elastic stiffness $k_e = 0.79k_g$, which corresponds with the upper-bound prediction of $I_e = 0.79I_g$ from the general method (Ibrahim and Adebar 2004). Up to a drift of about 1.5%, the reduction in stiffness was due to concrete cracking, and the effective stiffness of the wall compares well with the predicted lower-bound equal to 39% of the uncracked section stiffness.

In most cases, the actual response of a concrete wall will be somewhere between the upper-bound and lower-bound response. One possible approach would be to use the upper-bound effective stiffness in a force-based approach to make a safe estimate of force demand, and the lower-bound effective stiffness in a displacement-based approach to make a safe estimate of displacement demand. An alternative approach might be to relate effective stiffness to displacement level. If the displacements are small, the level of damage will be small and the effective stiffness will be close to the upper-bound value. If the displacements are large, there will be considerable damage and the effective stiffness will be closer to the lower-bound value. This approach is complicated by the fact that the effective stiffness in any cycle of loading depends on the maximum displacement in previous cycles. Thus the effective stiffness in the critical cycle depends on the magnitude of the preceding cycles. This suggests that the effective stiffness

depends on certain characteristics of the ground motion. In the current study, nonlinear dynamic analysis was used to study the influence of ground motions on the effective stiffness of high-rise cantilever walls.

Nonlinear Force-Displacement Model for High-Rise Cantilever Walls

A fibre model, the trilinear bending moment curvature relationship proposed by Adebar and Ibrahim (2002), and the results from the large-scale test of a cantilever wall (Adebar et al. 2007), were used to develop a simplified force–displacement model for high-rise cantilever walls. The model consists of a rational predefined envelope, and empirical hysteretic rules. These are briefly described separately below, and additional details can be found in Korchinski (2007).

Envelope

The envelope was defined from the results of a fibre model for a number of different high-rise cantilever walls. The simplified force-displacement relationship is linear before first cracking and then is nonlinear until the full section yields. As tension stiffening is included in the envelope, the section can be assumed to be perfectly plastic when the flexural capacity is reached, or a simple inclined linear segment can be used to model strain hardening of the reinforcement. A fourth order polynomial is used to represent the nonlinear segment of the curve. Five pieces of information are used to define the curve: position of start and endpoints, along with slope at both these points, and the position of an additional point on the curve. The definition of the curve is described further below.

The shear at cracking V_{cr} is a function of the cracking moment M_{cr}, and the distribution of lateral load acting on the wall. The corresponding displacement at first cracking Δ_{cr} can be calculated from first principles. The slope at the start of the nonlinear curve is reduced from the initial stiffness $k = V_{cr}/\Delta_{cr}$ to 0.9k. The shear at the flexural capacity of the wall V_N is a function of the flexural capacity M_N, and the distribution of lateral load acting on the wall. The displacement at flexural capacity Δ_{cr} is calculated by integrating curvatures determined from the bending moment diagram using the trilinear moment-curvature relationship for the wall. This process to determine displacement is repeated at $0.95(V_N-V_{cr})$ in order to determine the secant slope at the end of the nonlinear portion of the curve, and is repeated at $0.9(V_N-V_{cr})$ in order to determine the additional point that the curve is fit to. The five points required to describe the simplified force-displacement relationship are shown in Figure 1.

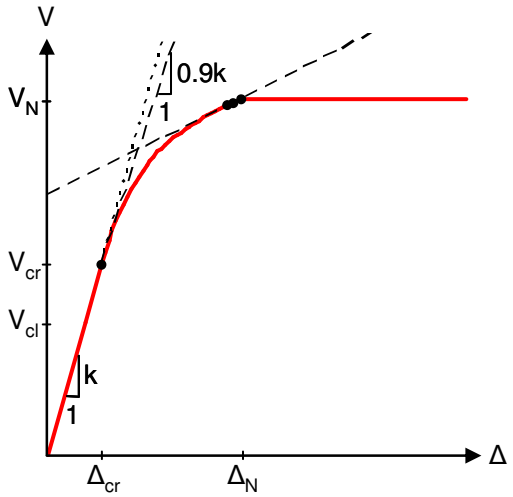

Figure 1. Simplified force-displacement relationship for a cantilever shear wall.

Hysteretic Model

The hysteretic rules that are combined with the envelope described above were developed empirically from the large-scale cantilever wall test conducted by Adebar et al. (2007). The wall is assumed to load

and unload along the initial linear curve with slope (stiffness) k until the shear is greater than the shear at first cracking V_{cr}. When the shear exceeds V_{cr}, the unloading path is linear from the point on the envelope to V_{cl} as shown in Fig. 2(a). V_l is calculated similarly to V_{cr} except that the concrete tension strength is assumed to be zero. That is, V_l is the portion of V_{cr} due to the axial compression from gravity loads.

Once the shear has exceeded V_{cr} in a previous cycle, reloading follows a linear path from V_{cr} to the point on the envelope at the maximum previous displacement. The reloading paths radiate from the point V_{cr}. The lower-bound reloading path extends from V_{cr} at a slope parallel to the lowest slope in the nonlinear segment of the envelope (see Fig. 2a) and intersects the yield plateau at a displacement Δ_{int} (see Fig. 2b). Once the maximum displacement exceeds Δ_{int}, all subsequent reloading follows the lower-bound trilinear reloading curve regardless of maximum displacement. The unloading paths continue to return linearly from the point on the envelope to V_{cl} (see Fig. 2b).

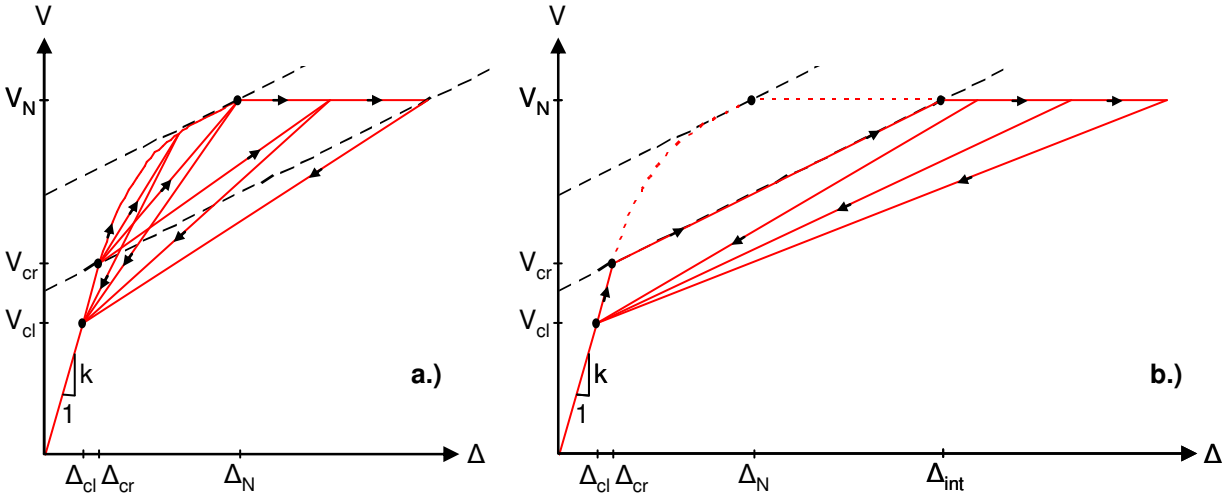

Figure 2. Trilinear force-displacement hysteretic model: (a) early stages, (b) later stages.

For mid-cycle reloading, the reloading path follows the initial slope k from the point where it leaves the unloading path (see Fig. 3). The reloading path intersects and follows a linear path from V_{cr} to the previous maximum displacement. When the maximum displacement exceeds Δ_{int}, mid-cycle reloading follows the initial slope k until rejoining the lower-bound reloading curve described above.

Computer program OpenSees (Open System for Earthquake Engineering Simulation) was used to conduct the nonlinear dynamic analysis for the current study. OpenSees is an open-source program in object-orientated C++ language. Most users perform numerical analysis in OpenSees using the Tcl scripting language. The object-oriented and open-source format allowed the model described above to be relatively easily implemented into a proven analysis program.

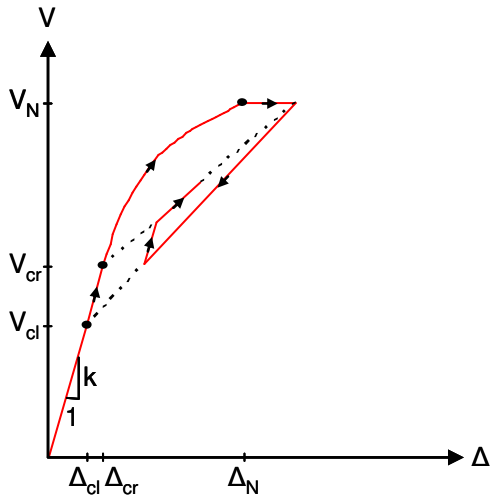

Figure 3. Mid-cycle reloading.

Nonlinear Dynamic Analysis

OpenSees has several existing material models such as elastic and elastic-perfectly-plastic (EPP) along with more specialized steel and concrete uniaxial material models. The basic framework for all material model subprograms implemented into OpenSees involves strain as input to the subprogram, and the resulting stress and tangent stiffness for the point on the stress-strain relationship is output from the subprogram. The strain is solved iteratively until equilibrium is reached. The framework can also be used with displacement input for force-displacement applications as was done in the current study. For the force–displacement model of cantilever shear walls described above, several history variables needed to be stored and updated in order to produce the proper loading or unloading behaviour.

The hysteretic model described above was used to model the large-scale cantilever wall tested by Adebar et al. (2007) as a single-degree-of-freedom system. The appropriate mass *m* was used in order to achieve an initial period of 2 and 4 seconds in the uncracked state. Mass proportional Rayleigh damping of 5% was used for all analysis.

The four ground motions selected for the nonlinear analysis were taken from the suite of ground motions used for calibration of the displacement modification procedure included within FEMA 440. The ground motions are for National Earthquake Hazard Reduction Program (NEHRP) site class C and site class D, and further information is provided in Table 1. The rationale for selecting these four ground motions was that they had a reasonably uniform increase in elastic spectral displacements in the 4 second period range.

Table 1. Characteristics of earthquake records.

Date	Earthquake	Magnitude (Ms)	Station name	PGA (cm/s^2)	PGV (cm/s)	PGD (cm)	NEHRP Site class
02/09/71	San Fernando	6.5	Pasadena, CIT Athenaeum	107.9	14.7	6.6	C
06/28/92	Landers	7.5	Yermo, Fire Station	240.3	57.5	37.5	C
10/17/89	Loma Prieta	7.1	Anderson Dam (downstream)	239.4	20.4	6.8	C
02/09/71	San Fernando	6.5	Vernon, Cmd Terminal	104.6	17.5	20.6	D

The ground motions were scaled so that the elastic demand on the cantilever wall with either a 2 sec or 4 sec initial period was R times the strength of the wall. The ground motions were scaled to give R = 1.5, 2, 2.5, 3, 4 and 5. Thus each ground motion was scaled to 12 different levels (6 R factors at 2 periods) resulting in a total of 48 different scaled ground motions.

In addition, a companion set of synthetic ground motions were created using computer program SYNTH. This program iteratively modifies the accelerogram until the acceleration spectrum matches the prescribed target spectrum. The target spectrum specified was an altered version of the National Building Code of Canada (NBCC) design spectrum for Vancouver, BC. The design spectrum was altered to be more representative of longer periods. The NBCC values of S_a for 2 and 4 seconds were used, but the decrease between them was taken proportional to 1/T as opposed to linear. This decrease proportional to 1/T was continued to T=6s when the decrease was set proportional to $1/T^2$ until T=10s. The NBCC uses the S_a for 4 seconds for all periods greater than 4 seconds. The alteration was done to reflect the levelling of spectral displacements for the longer periods. This levelling behaviour was observed in all four of the raw ground motions selected.

SYNTH calculates the acceleration spectrum for the raw accelerogram and determines the ratio between it and the target spectrum for a series of closely spaced periods specified by the user. This ratio is used to modify (increase or decrease) both the real and imaginary Fourier components of the accelerogram. An inverse Fourier transform is then performed on the altered components to create a new accelerogram. The entire process is repeated on each new accelerogram for a user specified number of iterations; this number was set at the recommended 10. SYNTH only changes the Fourier amplitude and does not change the Fourier phase spectrum because both the real and imaginary Fourier components are multiplied by the same ratio. This means that the strong motion duration of the initial accelerogram is maintained in the synthetic accelerogram. When examining the two accelerograms they appear quite similar with the “peaks” and “valleys” occurring in the same places but with different amplitudes. SYNTH is able to produce a ground motion that very closely follows the desired target spectrum. It is however important to select initial ground motions whose acceleration spectrums have similar shape to the target spectrum, primarily having peak accelerations occurring at similar periods. This limits the amount the initial ground motion needs to be altered. The selected raw ground motions have similarly shaped acceleration spectrums, as seen in Fig. 4. The synthetic ground motions were also scaled to give six different R values (1.5, 2, 2.5, 3, 4 and 5) at two different periods (2 and 4 sec) resulting in an additional 48 scaled ground motions.

Results from Analysis

For each of the 96 ground motions described above, a nonlinear analysis was conducted using the hysteretic model of the wall. A series of linear time step analyses were then conducted for a range of stiffness from the initial stiffness of the wall down to 20% of the initial stiffness at intervals of 1%. The mass, and Rayleigh damping of 5%, was kept constant over the range of decreasing stiffness. The maximum displacement for each record was plotted versus the period of the structure resulting in the well know elastic displacement spectrum (see Fig. 5).

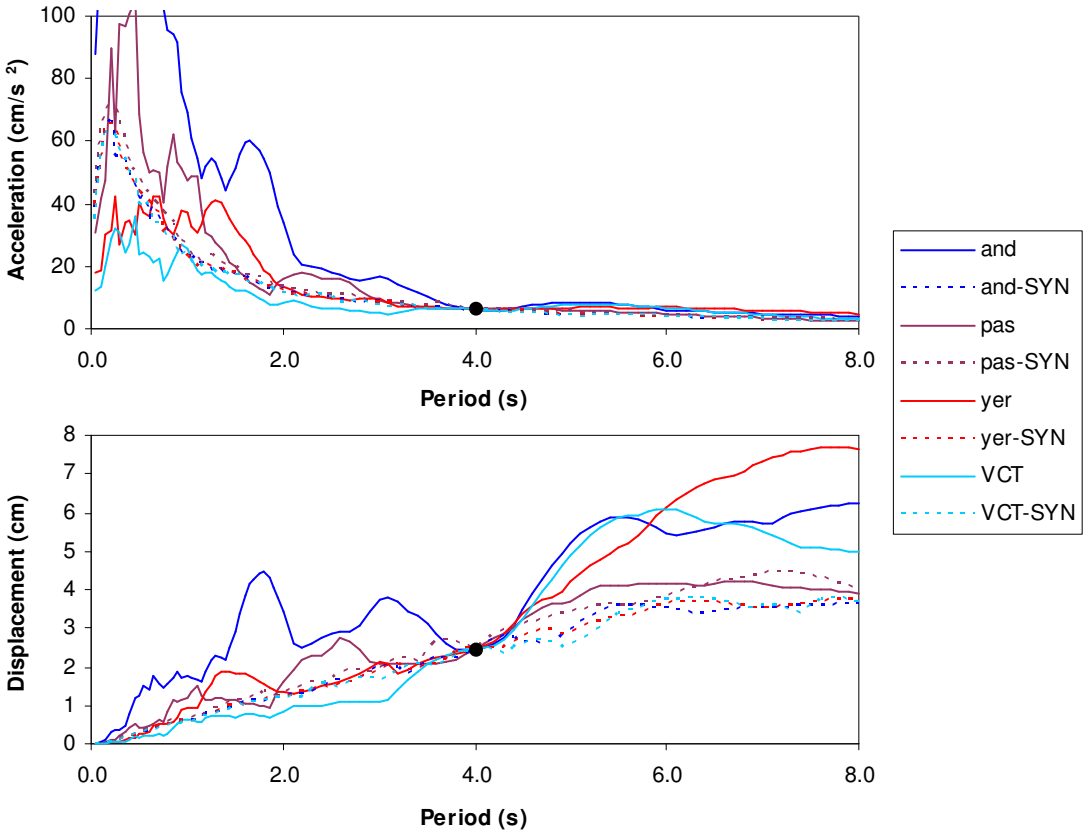

Figure 4. Acceleration and displacement spectrums of the scaled and synthetic (SYN) ground motions for an elastic system with a period of 4 seconds.

In addition, for each of the 96 ground motions, a series of nonlinear analyses were conducted using an elastic perfectly plastic model. The yield plateau was held constant at the capacity V_n of the wall, while the elastic portion of the elastic–plastic response was modified similar to the linear elastic analysis described above. That is, the elastic stiffness was reduced from the initial stiffness of the wall down to 20% of the initial stiffness at intervals of 1%. The maximum displacement for each nonlinear analysis was plotted versus the period of the structure calculated from the initial elastic range of response (see Fig. 5). The resulting displacement spectrum are very different than what is normally plotted for a bilinear response with a constant R factor as in current study, the strength of the elastic-plastic model was held constant and only the initial stiffness was reduced. As the initial stiffness reduces, the corresponding elastic force demand reduces, and the required strength for a given R factor reduces. The resulting spectrum from a bilinear analysis (with constant strength) is more erratic than the commonly produced inelastic spectrums for constant R.

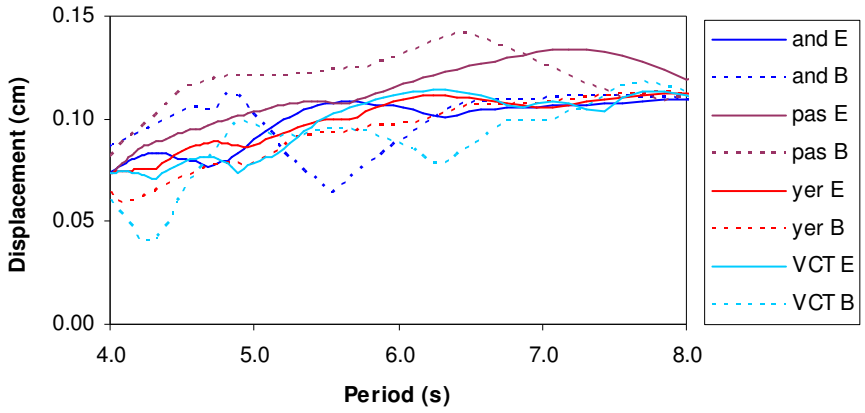

Figure 5. Typical displacement spectrums determined assuming linear-elastic (E) response, and using a bilinear (B) model. The examples shown are for synthetic ground motions with R = 3.0 based on an initial period of 4 sec.

The displacement determined from each linear and nonlinear analysis at reducing stiffnesses (increasing periods) was normalized by the displacement determined from the corresponding nonlinear model of the cantilever high-rise shear wall. Some typical results are shown in Fig. 6. The results are shown for the non-synthetic earthquake (left) and the synthetic earthquake (right), and for R = 1.5 (top) and R = 3.0 (bottom) based on the period of 4 sec.

The following observations can be made from the typical plots shown in Fig. 6. The difference between displacement ratios determined from the linear elastic response and bilinear response is less pronounced for R=1.5. The displacement ratios increase in a more uniform way when determined from a linear analysis than when determined from a bilinear analysis for constant strength. The synthetic ground motions give less erratic results compared to the non-synthetic ground motions. The displacement ratios determined from a linear elastic analysis using the synthetic ground motions seem to be the most useful for determining a relationship between predicted nonlinear displacement and stiffness reduction (increased period). Even with the synthetic ground motions scaled to the same initial R value, a large spread in displacement ratios is observed.

Conclusions

The important information contained in all the displacement ratio plots for the synthetic earthquakes are summarized in the two plots shown in Fig. 7. The point in the displacement ratio plots at which the line for a particular earthquake and analysis type crosses the line at a displacement ratio of 1.0, indicates the period that is needed to get the same displacement estimate as the nonlinear model for the high-rise cantilever wall. For example, the solid red line represents the results from different linear elastic analyses of the Yermo earthquake, while the red dashed line represents the results from different bilinear analyses of the Yermo earthquake. For the case of R = 1.5 and the synthetic earthquakes (top right plot in Fig. 6), the lines cross the 1.0 displacement ratio at periods of 4.32 s and 4.30 s, respectively. As the initial period of the structure is 4.0 s, the appropriate stiffness reduction factor $\alpha = k_e / k_g$ to be used for a linear elastic analysis and bilinear analysis (with constant strength) for this earthquake are 0.87 and 0.86, respectively. These results are plotted in the right-hand plot (for T = 4.0 s) in Fig. 7 at R = 1.5.

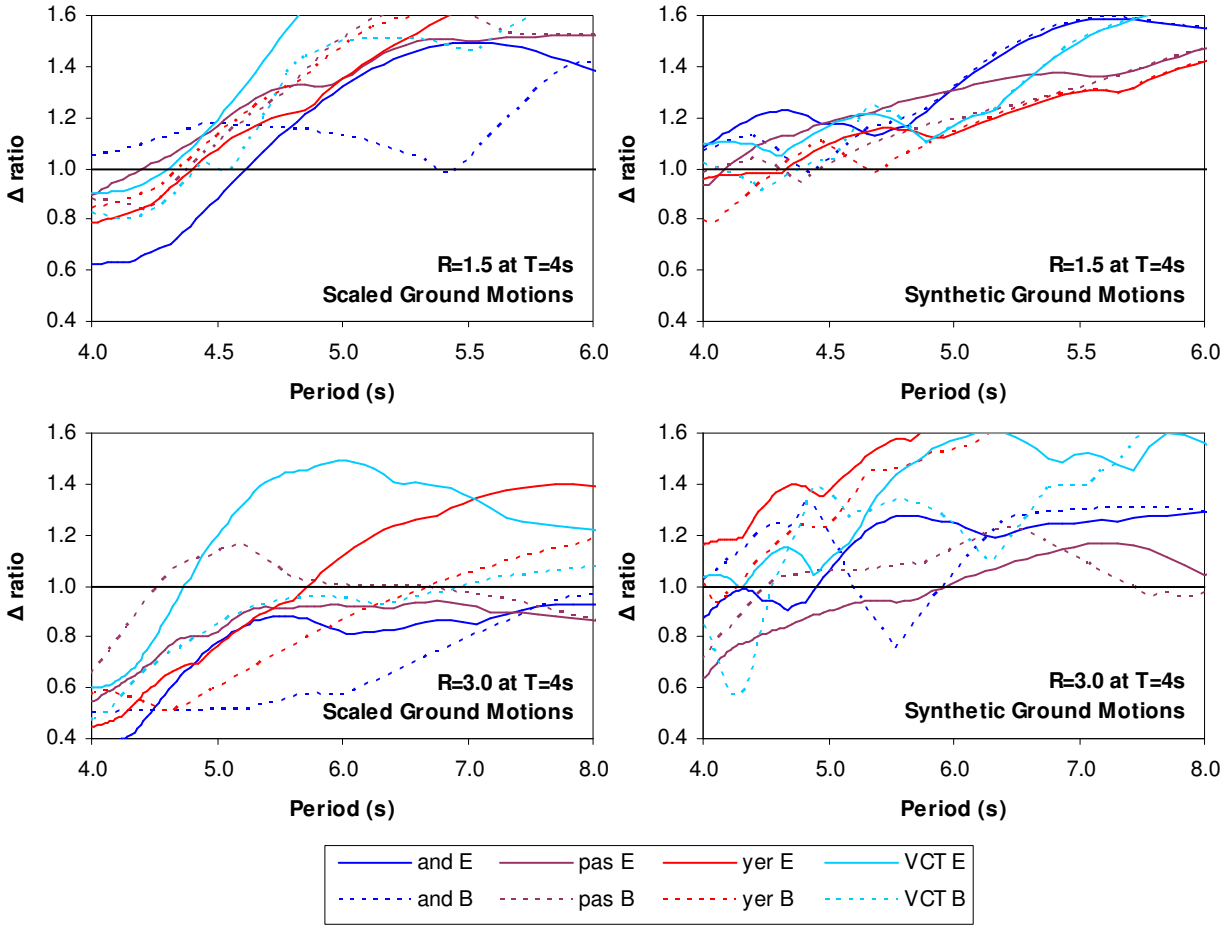

Figure 6. Example displacements determined from elastic analysis (E) and elastic-plastic analysis (B) nomalized by the displacement determined from nonlinear model of cantilever wall.

Fig. 7 shows all the results from the four synthetic earthquakes fit to National Building Code of Canada (NBCC) design spectrum for Vancouver, BC modified at the longer period range as described above. If the effective stiffness of the nonlinear wall model is determined from the elastic stiffness of an equivalent bi-linear load-displacement relationship with equal area-under-the-curve up to the point that the non-linear curves cross the nominal capacity, the stiffness reduction factor $\alpha = k_e/k_g$ should be taken as 80%. This corresponds reasonably well with the average of the results shown in Fig. 7. While the influence of the particular ground motions is very significant, the average results in Fig. 7 do suggest a trend, which is that the stiffness reduction factor $\alpha = k_e/k_g$ reduces gradually as the force reduction factor increases. For a structure where the stiffness of an uncracked wall results in a period of 2 sec, the trend is a gradual reduction from about 85% at R = 1.5 to a reduction factor of about 60% at an R = 5.0. For a taller wall where the stiffness of the uncracked wall results in a period of 4 sec, the trend is for a reduction factor of about 90% from R = 1.5 to about R = 2.5, and then a gradual decrease in the reduction factor to about 60% at R = 5.0.

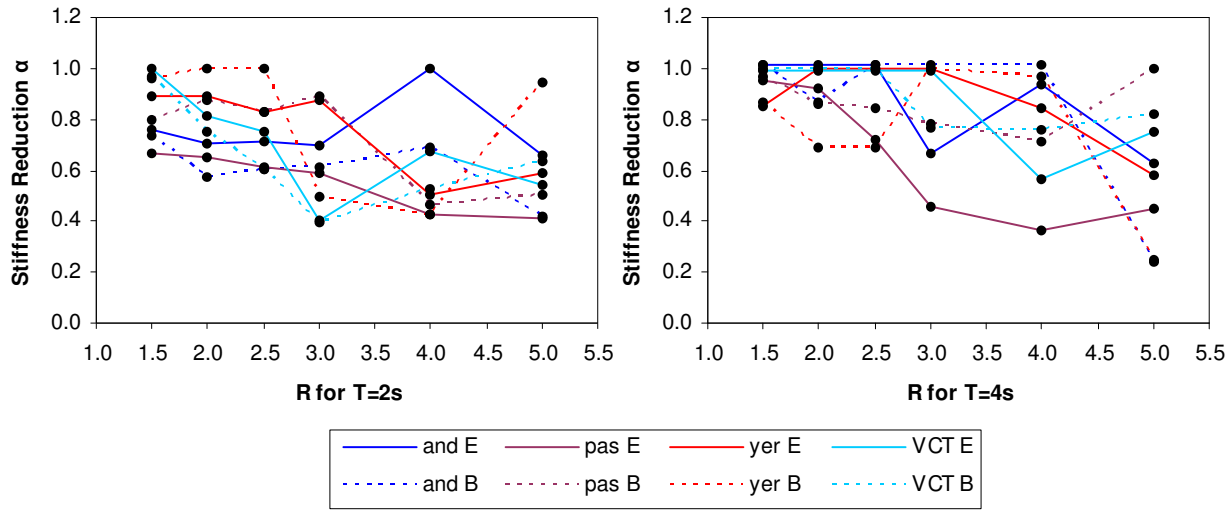

Figure 7. Stiffness reduction factors $\alpha = k_e / k_g$ versus force reduction factor R based on initial period for the four synthetic earthquakes.

References

Adebar, P., and Ibrahim, A.M.M., 2002. Simple Non-linear Flexural Stiffness Model for Concrete Shear Walls, Earthquake Spectra, EERI, 18(3), 407-426.

Adebar, P., Ibrahim, A.M.M., and Bryson, M., 2007. Test of a High-Rise Shear Wall: Effective Stiffness for Seismic Analysis, *ACI Structural Journal*. In press (to be published in 2007).

Ibrahim, A.M.M., and Adebar, P., 2004. Effective Flexural Stiffness for Linear Seismic Analysis of Concrete Walls, *Canadian Journal of Civil Engineering,* Vol. 31, No. 3, 597-607.

Korchinski, A. D., 2007. Nonlinear SDOF Approach to Determining the Effective Stiffness of High-Rise Concrete Shear Walls, *M.A.Sc. Thesis*, University of British Columbia, Vancouver.

Mattman, D. W., 2006. Inelastic Response of SDOF Systems Subjected to Subduction and Crustal Ground Motions, *M.A.Sc. Thesis*, University of British Columbia, Vancouver.

Naumoski, N. D., 2001. Program SYNTH Generation of Artificial Accelerograms Compatible with a Target Spectrum, *Computer Program and Supporting Documentation,* Carleton University, Ottawa.

Pacific Earthquake Engineering Research Center (PEER), 2006. Open System for Earthquake Engineering Simulation (OpenSees), *Computer Program and Supporting Documentation*, University of California, Berkeley.